Journal of Applied Mathematics and Physics (ZAMP)
Vol. 29, 1978 Birkhäuser Verlag Basel

Turbulent Boundary Layers with Large Streamline Curvature Effects

By Ronald M. C. So, Corporate Research and Development, General Electric Co., Schenectady, New York and George L. Mellor, Geophysical Fluid Dynamics Lab., Princeton University, Princeton, New Jersey, USA

1. Introduction

A goal in turbulent boundary layer research is to be able to calculate boundary layer development along any given surface under arbitrary free stream conditions. For two-dimensional plane flows, numerous calculation methods have been proposed by investigators in the past, and these have met with varying degrees of success [1]. All these methods, whether based on the integral or differential equations, are derived on the assumption that the static pressure variation across the boundary layer has very little effect on the flow and hence can be neglected. Measurements of two-dimensional turbulent boundary layers along plane surfaces lend support to this assumption [2]. However, when the methods are used to calculate rapidly growing boundary layers or flows along curved surfaces, they are found to be inadequate [1]. The reason is that existing two-dimensional methods neglect the effects of the curvature of the mean flow streamlines. This neglect is justifiable in laminar flows if $k\delta$ is small [3], where δ is the boundary layer thickness and k is the local longitudinal surface curvature. However, investigations on turbulent flows in curved channels [4–6] and along curved surfaces [6–14] showed that curvature of the mean flow not only gives rise to an appreciable change in the measured mean velocity and wall shear stress, but more importantly, it also gives rise to a substantial change in the turbulent flow structure [9–14]. The most striking effect of curvature was observed by So and Mellor [9, 10] who found that large convex curvature in the mean flow streamlines leads to vanishing shear stress in a region where the mean velocity gradient is still substantial. Therefore, it is evident that streamline curvature may not be a second order effect in turbulent flows. The effects of streamline curvature on turbulent flows are discussed thoroughly in a recent review article by Bradshaw [15] and the interested reader should refer to [15] for a more detailed discussion of these effects.

The importance of accounting for the streamline curvature effects in the prediction of two-dimensional turbulent flows was first pointed out by Prandtl [16]. His idea was later modified by Thompson [17] and extended by Bradshaw [18]. Thompson [17] argued that the primary effect of streamline curvature was on the entrainment process and he proceeded to modify Head's [19] entrainment function by

including curvature. With this modification, Thompson [17] found that good agreement was obtained between calculated values of displacement thickness, shape factor and skin friction coefficient and those measured by Schubauer and Klebanoff [20] on an aerofoil with $k\delta \simeq 0.007$ downstream of the pressure minimum.

On the other hand, Bradshaw [18] argued that the influence of streamline curvature is on the length scale. Using the analogy between buoyancy and centrifugal force to apply meteorological data to curved turbulent flows, Bradshaw [18] showed that the dissipation length scale was affected appreciably even though $k\delta \sim 0.003$. Bradshaw's [18] modification can be cast in a form similar to that proposed by Prandtl [16], whereby the mixing length is corrected for curvature effects through a multiplication factor F which is a function of a dimensionless curvature parameter. For small curvature, Bradshaw [18] proposed the use of the Monin–Oboukhov [21] formula for F which is

$$F = 1 - \beta Ri_c \tag{1}$$

where β is a free constant and Ri_c is the gradient Richardson number for curved shear flows, or

$$Ri_c = \frac{2kU}{\partial U/\partial y} \cdot \tag{2}$$

In (2), U is the mean velocity in the stream direction, k is the local surface curvature and y is the coordinate measured normal to the flow direction. Besides the data of Schubauer and Klebanoff [20], Bradshaw [15] also applied this correction to predict the measurements of Patel [7], Meroney and Bradshaw [12] and So and Mellor [9, 11] where $k\delta$ is 0.03, ± 0.01 and ± 0.16 respectively. The calculation method used is the same as that proposed by Bradshaw et al. [22], whereby a differential equation for the turbulent shear stress is solved simultaneously with the equations of mean motion. The boundary-layer equations are obtained by invoking the thin shear layer approximation which implies that the pressure variation in the normal direction is negligible. Using different values of β (7 for convex and 4 for concave surfaces), Bradshaw [15] obtained good correlation with the data of Patel [7], Meroney and Bradshaw [12] and Schubauer and Klebanoff [20]. However, substantial deviations were observed in the prediction of So and Mellor's [9, 11] measurements. In spite of this, the same correction formula was employed by Johnston and Eide [23] in their attempt to propose a simple method to calculate curved shear flows. Their calculation method is based on the flat plate boundary-layer equations and the turbulent shear stress is defined by Prandtl's mixing length argument. As a result, the only correction for curvature effects is in the mixing length. With $\beta = 6$, results obtained by Johnston and Eide [23] are similar to those obtained by Bradshaw [15].

Irwin and Arnot Smith [24] adopted a different approach to account for curvature effects. Instead of using (1) to correct for the Reynolds shear stress, they used the turbulence model of Launder et al. [25] to derive transport equations for the four Reynolds stresses for two-dimensional curved flows and an equation for the dissipation. Irwin and Arnot Smith [24] argued that since curvature of the mean flow

streamlines affects the turbulence structure more than the mean flow, it is justified to solve the transport equations simultaneously with the flat plate boundary-layer equations. This assumption limits the applicability of their method. With the exception of some curved wall-jet flows, their calculations showed good agreement with measurements up to $k\delta = \pm 0.01$ for boundary-layer flows. Again, the suitability of the method for flows with large curvature is in doubt.

An attempt to predict flows with large streamline curvature was made by Rastogi and Whitelaw [26]. They assumed the radius of curvature to be of the same order of magnitude as the boundary-layer thickness and obtained a set of equations for the mean flow that include the curvature terms and the variation of static pressure in the normal direction. To further account for curvature effects, they again applied (1) to the mixing length. They found that $\beta = 4.5$ gives the best agreement between calculated and measured curved wall-jet data up to $k\delta = 0.15$. However, when the method was used to predict curved boundary-layer flows, the result was not encouraging at all. Therefore, the question still remains as to how can the effects of large curvature be suitably accounted for in a relatively simple calculation method.

The present investigation addresses this question directly. To accomplish this objective, an approach based on a combination of the methods used by Irwin and Arnot Smith [24] and Rastogi and Whitelaw [26] is proposed. Turbulence modeling is used to derive an expression for the Reynolds shear stress for curved shear flows and this is used to close the two-dimensional curved boundary-layer equations obtained by So and Mellor [10] and Rastogi and Whitelaw [26]. In this approach, the thin shear layer approximation is not made and the empirical correction formula (1) proposed by Bradshaw [18] is not employed. However, it will be shown that, for small curvature, Bradshaw's correction formula can be recovered from the present approach. Therefore, the proposed method is equally applicable to flows with small as well as large streamline curvature effects.

2. The Boundary-Layer Equations

Consider a constant density, incompressible turbulent flow past a curved surface with local wall curvature $k = R^{-1}(x)$ where x is measured along the surface and R is the radius of curvature. The flow is assumed to be two-dimensional and steady in the mean. If an orthogonal coordinate system oxy attached to the surface is chosen (Figure 1(a)), then the boundary-layer equations obtained by assuming $|k\delta| \sim 0(1)$ can be written as

$$\frac{\partial U}{\partial x} + \frac{\partial V}{\partial y} + kV = 0 \tag{3}$$

$$U\frac{\partial U}{\partial x} + V\frac{\partial U}{\partial y} + kUV = -\frac{1}{\rho}\frac{\partial P}{\partial x} + \frac{\partial}{\partial y}\left(\frac{\tau}{\rho}\right) + 2k\left(\frac{\tau}{\rho}\right) \tag{4}$$

$$kU_p^2 = \frac{1}{\rho}\frac{\partial P}{\partial y} \tag{5}$$

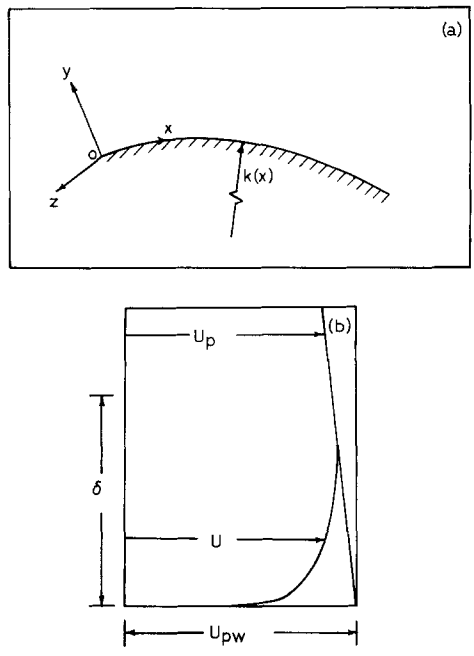

Figure 1
Coordinate system and a typical velocity profile.

where U, V are the mean velocity along x, y respectively, P is the mean static pressure, ρ is the fluid density, $U_p(x, y)$ is the potential velocity for curved flows (Figure 1(b)) and

$$\frac{\tau}{\rho} = -\overline{uv} + \nu\left(\frac{\partial U}{\partial y} - kU\right). \tag{6}$$

In (6), $-\overline{uv}$ is the Reynolds shear stress and ν is the kinematic viscosity of the fluid. The boundary conditions are taken to be the usual no slip condition at the wall and that the vorticity in the boundary layer must merge smoothly with the free stream vorticity at the edge of the layer which is considered zero. This last condition gives

$$\lim_{y\to\delta}\left(\frac{\partial U}{\partial y} + kU\right) = 0. \tag{7}$$

Alternatively, integrating (7) to give the potential velocity $U_p(x, y)$ outside the boundary layer, the outer boundary condition can be stated as:

$$\lim_{y\to\delta} U \to U_p(x, y) = U_{pw}(x)\, e^{-\kappa y} \tag{8}$$

where $U_{pw}(x)$ is recognized from classical boundary-layer theory as being the inviscid surface velocity (Figure 1(b)).

The set of equations (3)–(6) and (8) was derived by So and Mellor [10] based on asymptotic analysis similar to that presented by Yajnik [27], but more closely related to the analysis of Mellor [28]. This set of equations is used, instead of the

corresponding set derived by Rastogi and Whitelaw [26] through dimensional arguments, because it yields a relatively simple momentum integral balance. The von Karman momentum integral obtained from (3)–(5) with the appropriate boundary conditions is [9]

$$\frac{C_f}{2} = \frac{u_\tau^2}{U_{pw}^2} = \frac{d\theta}{dx} + (H+2)\frac{\theta}{U_{pw}}\frac{dU_{pw}}{dx} - q(x)\frac{dk}{dx} \tag{9}$$

where $u_\tau = (\tau_w/\rho)^{1/2}$ is the friction velocity, τ_w is the wall shear stress, C_f is the skin friction, $H = \delta^*/\theta$ is the profile shape factor and the integral parameters $\delta^*(x)$, $\theta(x)$, $q(x)$ are defined by

$$\delta^*(x) = \int_o^\infty \left(1 - \frac{U}{U_p}\right) dy \tag{10a}$$

$$\theta(x) = \int_o^\infty \frac{U}{U_p}\left(1 - \frac{U}{U_p}\right) dy \tag{10b}$$

$$q(x) = \int_o^\infty y\left(1 - \frac{U}{U_p}\right) dy + \int_o^\infty 2y\frac{U}{U_p}\left(1 - \frac{U}{U_p}\right) dy. \tag{10c}$$

A momentum integral similar to (9) can also be obtained from the set of equations used by Rastogi and Whitelaw [26] provided that an additional assumption is made concerning the pressure field [29]. In any event, it can be shown that the difference between the two momentum integrals is negligibly small, especially when k = constant and the Reynolds number of the flow is large. A detailed discussion of this is given by So [29]; therefore, it will not be repeated here.

3. The Shear Stress Equation

It was first demonstrated by So and Mellor [10] that the technique of turbulence modeling can be used to derive an expression for the Reynolds shear stress for two-dimensional flows over curved surfaces. The technique involved the use of appropriate models for the pressure-strain correlation and dissipation terms in the transport equations for the Reynolds stresses and the assumption of local equilibrium in the turbulence field. These simplifications reduce the transport equations to a set of algebraic equations for the Reynolds stresses which can be solved in terms of the mean flow quantities and surface curvature. This approach was later generalized to rotating curved flows by So [30]. In view of the fact that the details of the derivation have been previously given by So and Mellor [10] and So [30], only the result for the Reynolds shear stress is given. The interested reader should refer to the work of So and Mellor [10] and So [30] for more detailed discussion on the model.

The result obtained by So and Mellor [10] for the Reynolds shear stress, $-\overline{uv}$, can be written as

$$-\overline{uv} = \nu_{e_F}\left\{1 - \beta\frac{kU(\partial U/\partial y + kU)}{(\partial U/\partial y - kU)^2}\right\}^{3/2}\left|1 - \frac{kU}{\partial U/\partial y}\right|\left(\frac{\partial U}{\partial y} - kU\right) \tag{11}$$

where

$$\beta = \frac{72(l_1/\Lambda)}{1 - 6(l_1/\Lambda)} \tag{12}$$

$$\nu_{e_F} = (l_1\Lambda^{1/3})^{3/2}(1 - 6l_1/\Lambda)^{3/2}\left|\frac{\partial U}{\partial y}\right| \tag{13}$$

and l_1, Λ are length scales introduced through the turbulence models. From (11), it can be deduced that when $k = 0$

$$-\overline{uv} = \nu_{e_F}\left(\frac{\partial U}{\partial y}\right). \tag{14}$$

Therefore, ν_{e_F} is the eddy viscosity of a corresponding two-dimensional plane flow. In order to avoid empirical stipulation for l_1 and Λ, it is proposed to replace ν_{e_F} in (11) with the flat plate eddy viscosity function put forward by Mellor and Gibson [31][1]) and shown in Figure 2. Therefore, it remains to determine the ratio l_1/Λ and hence β in order to make (11) completely defined.

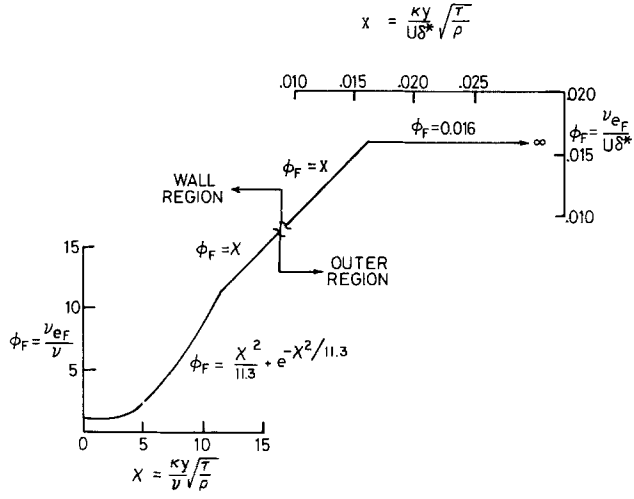

Figure 2
Flat plate eddy viscosity function of Mellor and Gibson [31].

So and Mellor [10] have shown that l_1/Λ can be easily determined from the wall-law region of two-dimensional plane flows. From the data of Laufer [33] and Klebanoff [34], they determined l_1/Λ to be 0.04 and from (12) β is approximated by 4. This value of β will be used for later calculation. The details of this derivation are given in [10], hence, they will not be repeated here.

[1]) The eddy viscosity function of Mellor and Gibson [31] involves combining the outer constant function of Clauser [32] with an inner wall function. Most other eddy viscosity functions which have appeared in the literature do not differ in principle or in practice, but they involve more empiricism than that proposed by Mellor and Gibson [31].

Another advantage in replacing ν_{e_F} with the flat plate eddy viscosity function of Mellor and Gibson [31] is that it allows the total shear stress, τ/ρ, to be written as

$$\frac{\tau}{\rho} = \nu_e\left(\frac{\partial U}{\partial y} - kU\right) \tag{15}$$

where

$$\nu_e = \nu_{e_F}\left[1 - \beta\frac{kU(\partial U/\partial y + kU)}{(\partial U/\partial y - kU)^2}\right]^{3/2}\left|\frac{\partial U}{\partial y} - kU\right|\Big/\left|\frac{\partial U}{\partial y}\right|. \tag{16}$$

Since ν_{e_F} approaches ν as $y \to o$ (Figure 2) and the correction factor in (16) approaches one, the correct behavior of τ/ρ as given by (6) is recovered. For large y, the viscous shear stress is negligible compared to the Reynolds shear stress and (15) reduces to (11) again.

Finally, it should be pointed out that for convex curvature, $\partial U/\partial y$ varies from positive at the wall to negative in the free stream because of (8). This gives rise to a singular behavior for ν_e inside the boundary layer. However, as later calculation shows, the quantity inside the square bracket in (16) goes to zero much faster than $\partial U/\partial y$ or $(\partial U/\partial y - kU)$. When that situation arises, ν_e vanishes and further integration of the equations is carried out with $\nu_e = \nu$ so that the condition of small viscous shear in the free stream can be satisfied. For concave surfaces, k is negative, and $\partial U/\partial y$ is always positive. Therefore, ν_e is well behaved across the boundary layer and approaches $2\nu_{e_F}$ in the free stream. Since $\nu_{e_F} \to 0.016U_p\delta^*$ for large y (Figure 2), it can be seen that ν_{e_F} is approximately constant in the free stream. As a result, τ/ρ does not vanish as $y \to \infty$. On the other hand, the terms $\partial(\tau/\rho)/\partial y + 2k(\tau/\rho) \sim 0$ as $y \to \infty$ which is evident from (4), (5) and (8). This situation is identical to that obtained in laminar flow except now τ/ρ takes on a larger value because $\nu_{e_F} > \nu$. In spite of this, later calculations show that the calculated velocity profiles are not very sensitive to the value of ν_{e_F} at large y.

4. Method of Solution

The method used to solve the set of equations (3)–(5) and (15) with no slip condition at the wall and outer boundary condition (8) is similar to that used by Mellor [35]. It is discussed in detail in [35] and the final equation to be solved is derived in [10]. Therefore, only a brief description of the method is given here.

The pressure term in (4) is eliminated by differentiating the integral of (5) and the velocity V and total shear stress τ/ρ are eliminated with the help of (3), (15) and (16). To further reduce the resultant partial differential equation to an ordinary differential equation in $f(x, \eta)$, where $\eta = y/\delta^*$ is a normalized y coordinate, a function $f'(x, \eta)$ is introduced, such that

$$f'(x, \eta) = \frac{\partial f}{\partial \eta} = \frac{U_p - U}{U_p}. \tag{17}$$

The final step is accomplished by applying the finite difference technique to the x coordinate. Thus reduced, the equation becomes an ordinary differential equation in η and can be written simply as

$$(b_5 f'')'_i = b_4 + b_3 f''_i + b_2 f'_i + b_1 f_i \tag{18}$$

where $f_i(x_i, \eta)$ is the value of f at x_i, primes denote differentiation with respect to η and the b's are functions of $\eta, f_{i-1}, \phi, \delta^*, U_{pw}, k$ and their derivatives. The eddy viscosity function $\phi = v_e/U_{pw}\delta^*$ can be written in terms of f as

$$\phi = \phi_F \left[1 + \beta \frac{k\delta^* f''(1 - f')}{\{f'' + 2k\delta^*(1 - f')\}^2} \right]^{3/2} \times \left| \frac{f'' + 2k\delta^*(1 - f')}{f'' + k\delta^*(1 - f')} \right| \tag{19}$$

where

$$\phi_F = \frac{v_{e_F}}{u_{pw}\delta^*} . \tag{20}$$

The boundary conditions at the wall are:

$$f'(x, o) = 1 \tag{21a}$$

$$f(x, o) = 0 \tag{21b}$$

and at the edge of the boundary layer is

$$\lim_{\eta \to \infty} f'(x, \eta) = 0. \tag{21c}$$

Thus simplified, the boundary-layer program of Herring and Mellor [36] can be used to numerically integrate (18) with respect to η subject to boundary conditions (21). The calculation can be initiated by either postulating an equilibrium profile as suggested by Mellor and Gibson [31] or using a measured profile as input. Prediction of the boundary layer development is obtained by carrying the calculation forward in step size of Δx once the pressure distribution on the surface is specified.

5. Small Curvature Results

It was pointed out by So [30] that (11) can be cast in a form similar to the Monin-Oboukhov formula for stratified flows. If a corresponding gradient Richardson number, Ri_c, is defined for curved shear flows such that

$$Ri_c = \frac{\text{Typical body force}}{\text{Typical inertia force}} \tag{22}$$

then it can be shown that [30]

$$Ri_c = \frac{2kU}{\dfrac{\partial U}{\partial y} - kU} \left[1 + \frac{2kU}{\dfrac{\partial U}{\partial y} - kU} \right]. \tag{23}$$

With this substitution and defining

$$l_o^2 = \left[(l_1 \Lambda^{1/3})\left(1 - \frac{6l_1}{\Lambda}\right)\right]^{3/2} \tag{24}$$

as the corresponding mixing length for plane flows, (11) can be written as

$$-\overline{uv} = l_o^2(1 - \tfrac{1}{2}\beta Ri_c)^{3/2}\left(\frac{\partial U}{\partial y} - kU\right)^2 . \tag{25}$$

Following Prandtl [16], the mixing length l_c for curved shear flows is given by

$$l_c^2 = l_o^2(1 - \tfrac{1}{2}\beta Ri_c)^{3/2}. \tag{26}$$

For very small k, (23) reduces to (2) and (26) reduces to the Monin–Oboukhov formula for the mixing length. As a result, the multiplication factor F as proposed by Bradshaw [18] is recovered. Also, for small Ri_c and with $\beta = 6$, (26) is exactly the same as the formula used by Rastogi and Whitelaw [26] for their prediction of curved wall jets.

The above argument is not limited to the turbulence model used by So and Mellor [10] and So [30]. It can be easily shown that if the assumption of local equilibrium in the turbulence field is made, the same small Ri_c result for l_c would be obtained with the use of a different turbulence model to close the Reynolds transport equations. As an example, consider the analysis of Irwin and Arnot Smith [24] who used the turbulence model proposed by Launder et al. [25] to close the Reynolds equations. In their original analysis, it is not assumed that turbulent production balances viscous dissipation in the thin shear layer. As a result, differential equations are obtained for the transport of Reynolds stresses. If the local equilibrium assumption is invoked, the differential equations can be reduced to simple algebraic equations for the Reynolds stresses, and the shear stress can again be solved in terms of the mean flow quantities and surface curvature. For small Ri_c, So [37] obtained the following result for the mixing length, namely

$$l_c = l_o(1 - 2.44Ri_c). \tag{27}$$

This agrees with the small Ri_c version of (26) with $\beta = 6$ and the correction formula used by Rastogi and Whitelaw [26]. Therefore, independent of the turbulence models used, the same result (with a disposable constant) is obtained in the case of small curvature for the mixing length for curved shear flows.

From the above discussion, it can be seen that the small Ri_c version of (26) is the same as the different correction formulae used by other investigators [15, 18, 23, 24, 26] to predict the effects of small streamline curvature. In view of this, the same result will be obtained if the small Ri_c version of (26) is used to calculate curved shear flows. It will also be shown later that the curvature terms in the mean flow equations have very little effect on the results as long as the shear stress is corrected for curvature effects as indicated by (11). Therefore, it remains to demonstrate the applicability of (26) for flows with large curvature effects.

6. Large Curvature Results

Measurements of boundary-layer flows on curved surfaces are scarce but an excellent summary of the published data is given by Bradshaw [15]. For convenience, part of this summary is given in Table I. The work of Clauser and Clauser [40] and

Table 1
Experiments on turbulent boundary layers on curved surfaces

Year	Investigators	Maximum $k\delta^{\dagger}$)	Pressure gradient*)
1930	Wilcken [38]	−0.2	z
1936	Schmidbauer [39]	+0.04	$f \rightarrow a$
1950	Schubauer and Klebanoff [20]	+0.02	a
1962	Tani [8]	?	z
1969	Patel [7]	±0.06	z
		±0.03	f
1972–1975	So and Mellor [9–11]	±0.16	z, a
1975	Meroney and Bradshaw [12]	±0.01	z

†) + convex curvature, − concave curvature.
*) a adverse, f favorable, z zero.

Liepmann [41, 42] is not included in Table I because the investigations deal mainly with transition from laminar to turbulent flows. With the exception of Wilcken [38] and So and Mellor [9–11], all the experiments tabulated in Table 1 were carried out on surfaces with very small longitudinal curvature. The only complete set of measurements with large curvature effects is that obtained by So and Mellor [9–11]. Their data is very well documented and hence, is suitable for verification of calculation methods. On the other hand, it is very difficult to extract meaningful data from the reported measurements of Wilcken [38] for comparison purposes. In view of this, the decision is made to compare the present calculations with the measurements of So and Mellor [9–11] only. Due to reasons discussed in Section 5, a comparison with small curvature measurements will not be given.

For convex curvature, two cases are chosen; zero pressure gradient flow [9] and separating flow [10]. The wall static pressure distributions along the test wall for these two cases are given in Figure 3. The convex surface has longitudinal radii of curvature that vary from 25.4 cm at the entrance ($x = 122$ cm) to 35.2 cm at the exit ($x \simeq 210$ cm) of the curved test section. For the zero pressure gradient flow case, $k\delta$ varies from 0.09 to 0.07 while for the separating flow case $k\delta$ varies from 0.08 to 0.18. Calculations are also made to show the drastic effect of curvature by assuming the same initial and boundary conditions but letting $k \rightarrow 0$.

For concave curvature, comparisons are made with zero pressure gradient flow only [11]. The wall static pressure distribution along the concave test wall is given in Figure 4. Since the concave surface has longitudinal radii of curvature that vary from −40.6 cm at the entrance ($x = 152.4$ cm) to −61.2 cm at the exit ($x = 310$ cm) of the

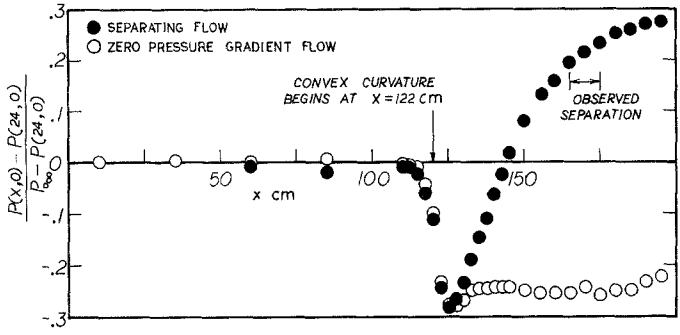

Figure 3
Wall static pressure distribution for zero pressure gradient and separating flows on a convex surface. $P(x, 0)$ is the wall static pressure, $P(24, 0)$ is the wall static pressure at $x = 24$ cm and $P_{o\infty}$ is the total pressure in the tunnel.

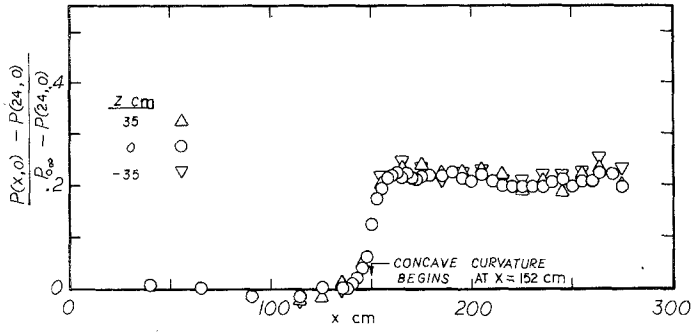

Figure 4
Wall static pressure distribution for zero pressure gradient flow on a concave surface. The meanings of the various P are the same as those given in Figure 3.

curved test section, the average $k\delta$ varies from -0.11 at $x = 178$ cm to -0.16 at $x = 244$ cm. The measurements of So and Mellor [11] reveal that the boundary layer development at two spanwise locations is different because of the presence of a system of longitudinal vortices, therefore, the two-dimensional calculations are compared with the "average" measurements only.

The initial conditions chosen for all calculations are the measurements obtained by So and Mellor [9–11] at $x = 61$ cm. Hence, all calculations begin on a flat surface and proceed on to a curve surface.

Zero Pressure Gradient Flow on a Convex Wall

The calculated results are given in Figures 5 to 7 and the agreement among the various integral parameters θ, δ^* and H is shown to be very good (Figure 5). It can be seen that the effect of convex curvature is to reduce θ and increase δ^*. As a result, H is very much different from the corresponding flow along a flat plate. Although the

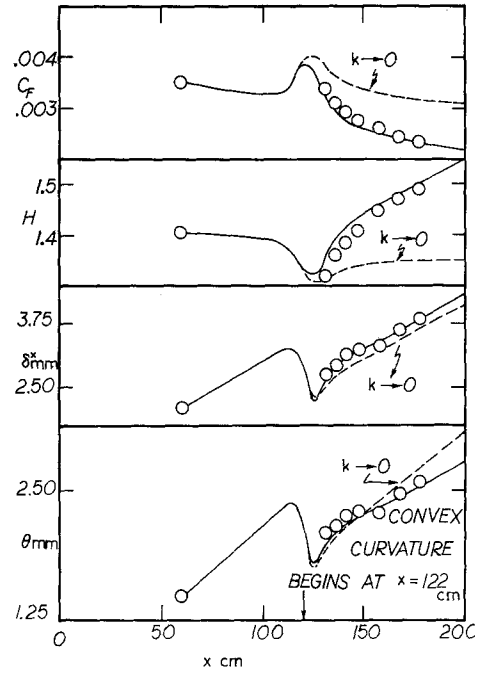

Figure 5
Comparison of calculated and measured skin friction, shape factor, displacement and momentum thicknesses for zero pressure gradient flow on a convex surface.

calculation shows that $H \rightarrow 1.35$ when the flow is in equilibrium again after passing through the favorable pressure gradient in the case of $k \rightarrow 0$, no equilibrium is reached in the case of finite curvature. The prediction of C_f is excellent. On the other hand, if $k = 0$ is assumed in the prediction scheme, the calculated skin friction is generally 25% higher than the measured values. This indicates that turbulent flows along convex surface cannot support as high an adverse pressure gradient as the same flow over a flat surface.

Calculated velocity profiles at $x = 133.5$, 150, 170.2 and 180.3 cm are shown in Figure 6 together with the measured profiles. In general, agreement is good, and the present method predicts the velocity profile accurately even at $x = 133.5$ cm which is immediately downstream of the strong favorable pressure gradient.

The present method also predicts the shear stress profile correctly (Figure 7), especially the point where the shear stress vanishes. Near the wall the agreement is off, but in this region there is strong evidence to indicate that the measurements are in error due to finite wire effects in regions of high shear (Bissonnette and Mellor [43]). Outside of this region ($y \leq \delta^*$ approximately), the agreement is very good. The shear stress profile of the $k \rightarrow 0$ calculation at $x = 150$ cm is also shown which clearly illustrates the effect of large convex curvature in 'turning off' shear stress.

Calculations were also made to determine the significance of the curvature terms

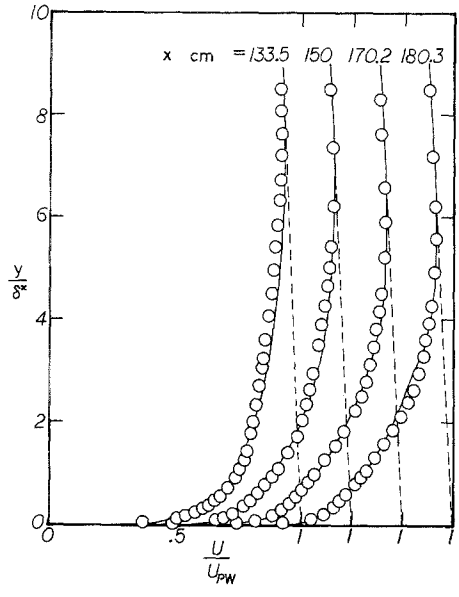

Figure 6
Comparison of calculated and measured mean velocity profiles for zero pressure gradient flow on a convex surface.

in the mean equations of motion. In these calculations, the flat plate equations were used in conjunction with the eddy viscosity given in (16). The results are essentially the same as those shown in Figures 5 to 7 and show that the effect of curvature on the mean flow is small compared to its effect on the turbulent structure. This last point has also been convincingly demonstrated by So [29] who used the integral approach to predict curved boundary-layer flows and found substantial differences between calculated and measured C_f.

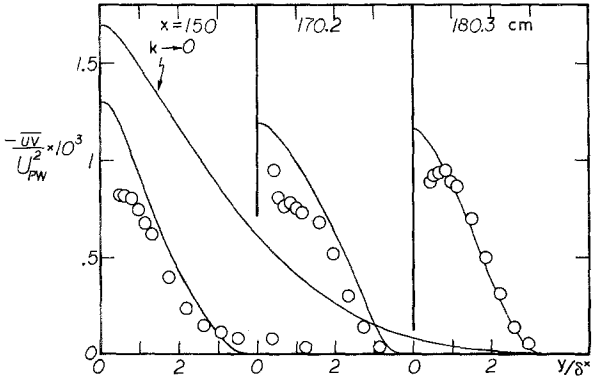

Figure 7
Comparison of calculated and measured shear stress profiles for zero pressure gradient flow on a convex surface.

Separating Flow on a Convex Wall

In calculating the separating flow, the measured potential velocity distribution at the wall up to $x = 159$ cm is used, but from $x = 159$ cm to $x = 190$ cm, the extrapolated distribution is used (Figure 8). It is believed that this will give a better prediction of the separation point. As in the case of zero pressure gradient flow, additional calculations with $k \to 0$ are made to demonstrate the drastic effect of curvature.

The calculated and measured θ and δ^* are given in Figure 9. Under the influence of

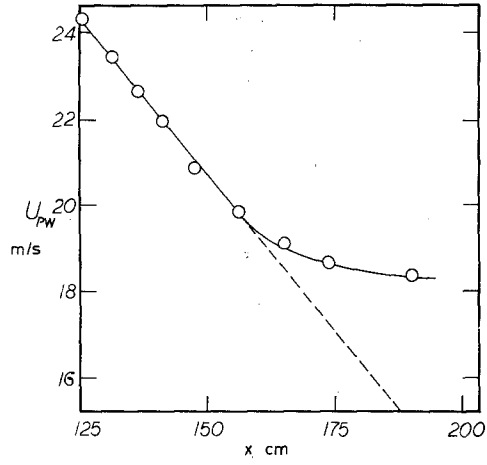

Figure 8
Distribution of potential velocity at the wall for separating flow on a convex surface.

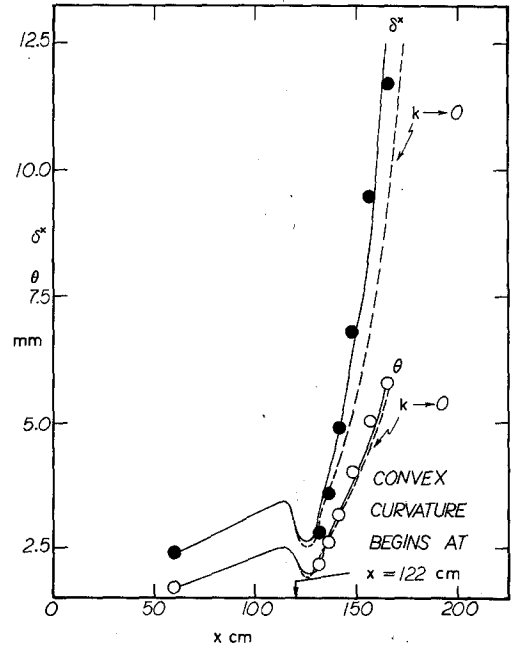

Figure 9
Comparison of calculated and measured displacement and momentum thicknesses for separating flow on a convex surface.

adverse pressure gradient, the difference in the development of θ is unnoticeable. However, the difference in δ^* is discernible, especially near separation.

Although the location of the point of separation is not known exactly, it is believed that the flow separates somewhere between $x = 167.5$ cm and $x = 178$ cm. If separation is defined as the point where $C_f \to 0$, then the separation point as calculated by the present method is at $x = 170$ cm (Figure 10). With zero wall curvature, the flow does not separate until $x = 203$ cm. This supports the previous conclusion that under the same distribution of potential velocity at the wall, the flow separates earlier when the surface has a finite curvature.

As seen in Figure 10, the calculated C_f agrees well with the measured C_f up to x

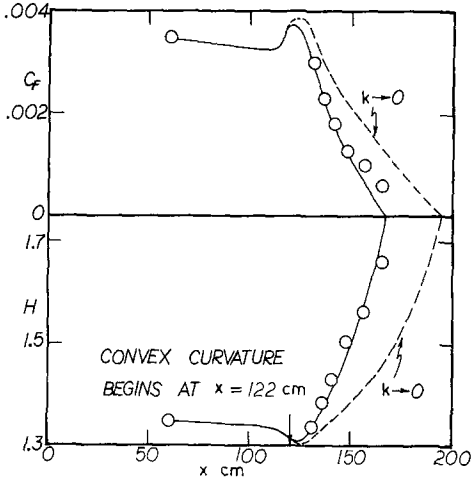

Figure 10
Comparison of calculated and measured skin friction and shape factor for separating flow on a convex surface.

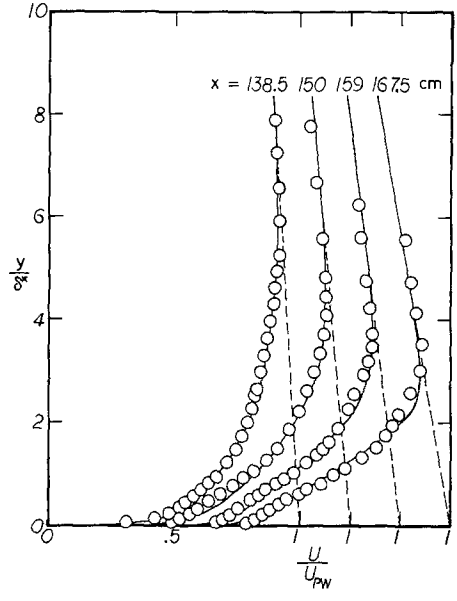

Figure 11
Comparison of calculated and measured mean velocity profiles for separating flow on a convex surface.

$= 150$ cm but after this the calculated value is lower. The reason is that in the actual flow, the inviscid-viscous interaction causes the velocity distribution to level off, and therefore, has a delaying effect on separation. This is borne out by the fact that if the measured velocity distribution up to $x = 190$ cm is used, the calculation will give good agreement with C_f up to $x = 167.5$ cm. However, separation is predicted to be at $x = 198$ cm, and no separation is predicted for the $k \to 0$ calculation.

The agreement between calculated and measured velocity profiles at $x = 138.5$, 150, 159 and 167.5 cm is also very good (Figure 11). However, the agreement between calculated and measured shear stress profiles (Figure 12) is poorer than the zero

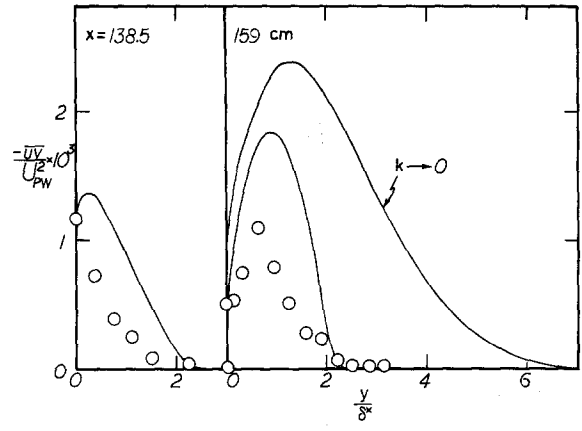

Figure 12
Comparison of calculated and measured shear stress profiles for separating flow on a convex surface.

pressure gradient case; but the point where $\tau \to 0$ is accurately predicted. Even though the flow is under the influence of a strong adverse pressure gradient, the shear stress still vanishes at about half the boundary layer thickness. Again, this demonstrates the strong effects of large curvature on the flow structure.

Zero Pressure Gradient Flow on a Concave Wall

The comparison of calculated and measured results for flow on a concave wall is given in Figures 13 and 14. From Figure 13, it can be seen that the calculated and

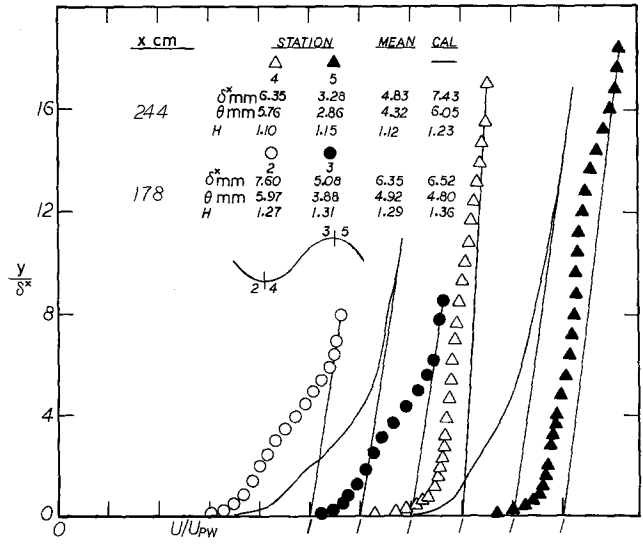

Figure 13
Comparison of calculated and measured velocity profiles for zero pressure gradient flow on a concave surface.

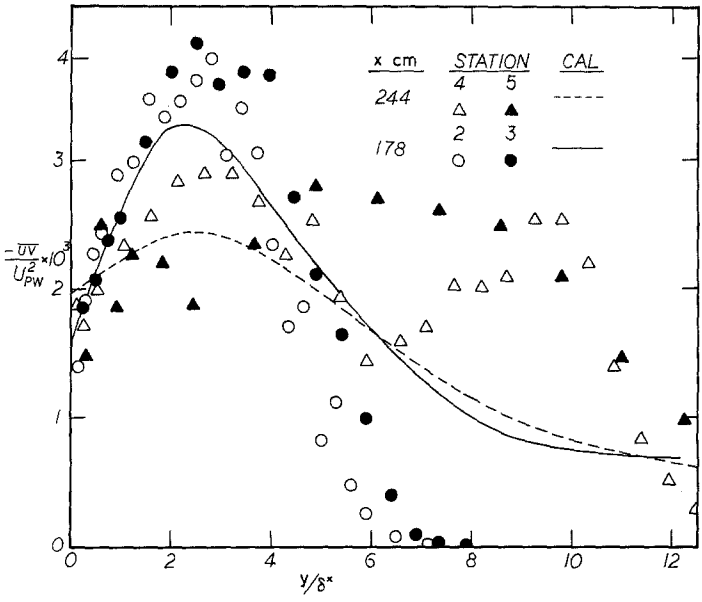

Figure 14
Comparison of calculated and measured shear stress profiles for zero pressure gradient flow on a concave surface.

'average' measured δ^*, and H compare favourably at $x = 178$ cm but deviate by about 45% at $x = 244$ cm. In spite of this, the shape of the profile compares favourably. The calculated wall shear stresses at the two x locations agree well with the 'average' extrapolated values of the measured shear stress profiles (Figure 14), but disagree with the wall shear stresses determined from the mean velocity profiles [11]. Since the latter was determined by assuming the existence of a log-law region near the wall, its reliability is in doubt. On the other hand, the present calculated C_f values at $x = 178$ cm and 244 cm are 0.0032 and 0.0040, respectively and agree with the results of Bradshaw [15]. Therefore, it can be concluded that the present method gives a fair prediction of the integral parameters of the 'average' flow over a concave wall with large curvature.

To summarize, it can be said that the present approach correctly predicts the effects of large convex curvature, especially the behavior of the Reynolds shear stress. Also, the calculated results are in better agreement with measurements compared to the other approaches reported in the literature [15, 18, 23, 26].

7. The Combined Effects of Curvature and Rotation

Surface curvature gives rise to an external body force in the mean flow equations and this depends on the U-component of velocity. If a flow in a rotating environment is considered such that the axis of rotation is normal to the plane of flow, then the mean flow is subject to the influence of a Coriolis force. Since the Coriolis force is also

dependent on the U-component of velocity, it is reasonable to expect the effects of rotation on turbulent flow to be similar to those due to surface curvature. This observation is borne out by the analytical result obtained by So [30] who derived the following expression for the Reynolds shear stress for a rotating curved flow:

$$-\overline{uv} = l_o^2[1 - \tfrac{1}{2}\beta(Ri_c + Ri_r + 2S_cS_r)]^{3/2}\left(\frac{\partial U}{\partial y} - \frac{kU}{h}\right)^2. \tag{28}$$

In (28), Ri_r is the gradient Richardson number for rotating flows and is defined as:

$$Ri_r = S_r(1 + S_r) \tag{29a}$$

where

$$S_r = \frac{-2\Omega}{\dfrac{\partial U}{\partial y} - \dfrac{kU}{h}} \tag{29b}$$

$$S_c = \frac{2kh^{-1}U}{\dfrac{\partial U}{\partial y} - \dfrac{kU}{h}} \tag{29c}$$

and Ω is the constant speed of rotation, $h = 1 + ky$ is the metric coefficient. If $h = 1$ is assumed and $\Omega = 0$, then $S_r = 0$ and (28) reduces to (11). On the other hand, if $k = 0$, it can be seen that (28) also reduces to a form similar to (11). This shows that Coriolis force has the same effect on turbulent shear stress as surface curvature.

In the analysis of Johnston and Eide [23], the combined effects of rotation and surface curvature are assumed to be additive. From (28), it can be seen that this is true only for small values of the respective Richardson numbers. If the effects of surface curvature and rotation are small, then $S_c \ll 1$, $S_r \ll 1$ and $Ri_c \simeq S_c$, $Ri_r \simeq S_r$. With this simplification, the mixing length l for rotating curved flows is given by

$$l = l_o[1 - \tfrac{3}{8}\beta(Ri_c + Ri_r)] \tag{30}$$

which is the same as the expression proposed by Johnston and Eide [23]. The validity of (30) for small Ri_c or Ri_r has been demonstrated by Johnston and Eide [23], therefore, there is no need to repeat the calculation. Besides, good rotating flow data are scarce and very little new information can be added to those already presented by Johnston and Eide [23].

On the other hand, for moderate to large values of Ri_c and Ri_r, (28) clearly shows that the effects of rotation and surface curvature are not additive. However, So [30] has shown that for such flows (28) can be reduced to a form similar to (11) by defining a combined gradient Richardson number, Ri, such that

$$Ri = (S_c + S_r)(1 + S_c + S_r) \tag{31}$$

In other words, (16) will remain the same provided that $kU(\partial U/\partial y + kU)/(\partial U/\partial y$

$-kU)^2$ is replaced by $Ri/2$. As a result, the present method is also applicable to rotating curved flows with large rotation and surface curvature effects. Unfortunately, lack of test data prevents the presentation of a convincing comparison.

From the above discussion, it can be seen that the present approach is not just limited to curved flows. It can also be applied to rotating plane flows and two-dimensional rotating curved flows with both small and large external body force effects. Again, for small external body force effects, the approach reduces to the more familiar method put forward by other investigators [15, 18, 23]. Therefore, the main finding of the present study is that it is possible to extend those methods to account for large rotation and surface curvature effects.

8. Conclusions

With the assumption of local equilibrium in a turbulent field and the introduction of suitable turbulence models in the curved flow transport equations for the Reynolds stresses, an expression is obtained for the shear stress in terms of the mean flow quantities, surface curvature and a flat plate eddy viscosity function. This relation is used to close the mean flow equations for curved shear flows. The present approach demonstrates that the primary influence of streamline curvature is in the turbulent structure, while the additional curvature terms in the mean flow equations are shown to be unimportant. The calculated results also show that the present method accurately predicts the boundary-layer growth, the skin friction, the mean velocity profiles, the shear stress distribution and the point where the shear stress vanishes for turbulent boundary-layer flows over surfaces with large longitudinal curvature under arbitrary free stream conditions. For flows with small curvature effects, the shear stress equation is reduced to the familiar Monin–Oboukhov formula and the present method is shown to reduce to other more familiar methods used by various investigators. Therefore, the present approach is more general in that it applies to flows with small as well as large curvature effects.

The shear stress relation is shown to be independent of the turbulence models used because the same relation (with a disposable constant) can be obtained from Irwin and Arnot Smith's [24] analysis.

The present method can also be applied to predict the effects of Coriolis force on the development of turbulent boundary layers. Corrections for the Reynolds shear stress is again given by the relation derived by So [30]. For small Coriolis force effects, the equation reduces to the familiar Monin–Oboukhov formula used by other investigators [15, 18, 23]. As a result, the present approach is suitable for flows with combined curvature and Coriolis force effects.

Acknowledgement

This work was funded by NASA Grant, NGR 31-001-074 monitored by Mr. S. Lieblein. Also, use was made of computer facilities made available by the Geophysical Fluid Dynamics Laboratory at Princeton.

References

[1] S. J. KLINE, M. V. MORKOVIN, G. SOVRAN and D. J. COCKRELL (eds.), *Proc. Stanford Conf. on Computation of Turbulent Boundary Layers*, Vol. I, AFOSR-IFP (1968).

[2] D. E. COLES and E. A. HIRST (eds.), *Proc. Stanford Conf. on Computation of Turbulent Boundary Layers*, Vol. II, AFOSR-IFP (1968).

[3] M. VAN DYKE, *Higher Approximations in Boundary Layer Theory, Part I: General Analysis*, J. Fluid Mech. *14*, 161–177 (1962); also *Part II: Application to Leading Edges*, J. Fluid Mech. *14*, 481–495 (1962).

[4] F. L. WATTENDORF, *A Study of the Effect of Curvature on Fully Developed Turbulent Flow*, Proc. Roy. Soc. *A148*, 565–598 (1934).

[5] S. ESKINAZI and H. YEH, *An Investigation of Fully Developed Turbulent Flows in a Curved Channel*, J. Aero. Sci. *23*, 23–34 (1956).

[6] L. B. ELLIS and P. N. JOUBERT, *Turbulent Shear Flow in a Curved Duct*, J. Fluid Mech. *62*, 65–84 (1974).

[7] V. C. PATEL, *The Effects of Curvature on the Turbulent Boundary Layer*, Aero. Res. Counc. R. & M. 3599 (1969).

[8] I. TANI, *Production of Longitudinal Vortices in the Boundary Layer Along a Concave Wall*, J. Geophys. Res. *67*, 3075–3080 (1962).

[9] R. M. C. SO and G. L. MELLOR, *Experiment on Convex Curvature Effects in Turbulent Boundary Layers*, J. Fluid Mech. *60*, 43–62 (1973).

[10] R. M. C. SO and G. L. MELLOR, *An Experimental Investigation of Turbulent Boundary Layers Along Curved Surfaces*, N.A.S.A. Contractor Rept. No. 1940 (1972).

[11] R. M. C. SO, and G. L. MELLOR, *Experiment on Turbulent Boundary Layer on a Concave Wall*, Aero. Quart. *26*, 25–40 (1975).

[12] R. N. MERONEY and P. BRADSHAW, *Turbulent Boundary Layer Growth over a Longitudinally Curved Surface*, AIAA J. *13*, 1448–1453 (1975).

[13] D. P. MARGOLIS and J. L. LUMLEY, *Curved Turbulent Mixing Layer*, Phys. Fluids *8*, 1775–1784 (1965).

[14] I. P. CASTRO and P. BRADSHAW, *The Turbulence Structure of a Highly Curved Mixing Layer*, J. Fluid Mech. *73*, 265–304 (1976).

[15] P. BRADSHAW, *Effects of Streamline Curvature on Turbulent Flow*, AGARDograph No. 169 (1973).

[16] L. PRANDTL, *Einfluss stabilisierender Kräfte auf die Turbulenz*, Sonderdruck Vorträge aus dem Gebiete der Aerodynamik und verwandter Gebiete, Aachen (1929); Translation N.A.C.A. TM-625.

[17] B. G. J. THOMPSON, *A New Two-parameter Family of Mean Velocity Profiles for Incompressible Turbulent Boundary Layers on Smooth Walls*, Aero, Res. Counc. R & M 3463 (1967).

[18] P. BRADSHAW, *The Analogy Between Streamline Curvature and Buoyancy in Turbulent Shear Flow*, J. Fluid Mech. *36*, 177–191 (1969).

[19] M. R. HEAD, *Entrainment in the Turbulent Boundary Layer*, Aero Res. Counc. R & M 3152 (1958).

[20] G. B. SCHUBAUER and P. S. KLEBANOFF, *Investigation of Separation of the Turbulent Boundary Layer*, N.A.C.A. Rept. No. 1030 (1951).

[21] A. S. MONIN and A. M. OBOUKHOV, *Basic Turbulent Mixing Laws in the Atmospheric Surface Layer*, Trudy. Geofiz. Inst. An. SSSR, *24*, 163–187 (1954).

[22] P. BRADSHAW, D. H. FERRISS and N. P. ATWELL, *Calculation of Boundary Layer Development Using the Turbulent Energy Equation*, J. Fluid Mech. *28*, 593–616 (1967).

[23] J. P. JOHNSTON and S. A. EIDE, *Turbulent Boundary Layers on Centrifugal Compressor Blades: Prediction of the Effects of Surface Curvature and Rotation*, J. Fluids Eng. Trans. ASME *98*, 374–381 (1976).

[24] H. P. A. H. IRWIN and P. ARNOT SMITH, *Prediction of the Effect of Streamline Curvature on Turbulence*, Phys. Fluids *18*, 624–630 (1975).

[25] B. E. LAUNDER, G. J. REECE and W. RODI, *Progress in the Development of a Reynolds Stress Turbulence Closure*, J. Fluid Mech. *68*, 537–566 (1975).

[26] A. K. RASTOGI and J. H. WHITELAW, *Procedure for Predicting the Influence of Longitudinal Curvature on Boundary Layer Flows*, ASME Paper No. 71-WA/FE-37 (1971).

[27] K. S. YAJNIK, *Asymptotic Theory of Turbulent Shear Flows*, J. Fluid Mech. *42*, 411–427 (1970).

[28] G. L. MELLOR, *The Large Reynolds Number Asymptotic Theory of Turbulent Boundary Layers*, Int. J. Eng. Sci. *10*, 851–873 (1972).

[29] R. M. C. SO, *Momentum Integral for Curved Shear Layers*, J. Fluids Eng. Trans. ASME *97*, 253–256 (1975).

[30] R. M. C. SO, *A Turbulence Velocity Scale for Curved Shear Flows*, J. Fluid Mech. *70*, 37–57 (1975).

[31] G. L. MELLOR and D. M. GIBSON, *Equilibrium Turbulent Boundary Layers*, J. Fluid Mech. *24*, 225–252 (1966).

[32] F. H. CLAUSER, *The Turbulent Boundary Layer*, Adv. Appl. Mech. *4*, 1–51 (1956).

[33] J. LAUFER, *The Structure of Turbulence in Fully Developed Pipe Flow*, N.A.C.A. Rept. No. 1174 (1954).
[34] P. S. KLEBANOFF, *Characteristics of Turbulence in a Boundary Layer with Zero Pressure Gradient*, N.A.C.A. Rept. No. 1247 (1955).
[35] G. L. MELLOR, *Incompressible Turbulent Boundary Layers with Arbitrary Pressure Gradients and Divergent or Convergent Cross Flows*, AIAA J. *5*, 1570–1579 (1967).
[36] H. J. HERRING and G. L. MELLOR, *A Computer Program to Calculate Incompressible Laminar and Turbulent Boundary Layer*, N.A.S.A. Contractor Rept. No. 1564 (1968).
[37] R. M. C. SO, *Discussion on Turbulent Wall Jets With Cylindrical Streamwise Surface Curvature*, J. Fluids Eng. Trans. ASME *98*, 780–782 (1976).
[38] H. WILCKEN, *Turbulente Grenzschichten an gewölbten Flächen*, Ing.-Arch. *1*, 357–376 (1930).
[39] H. SCHMIDBAUER, *Behaviour of Turbulent Boundary Layers on Curved Convex Wall*, N.A.C.A. TM-791 (1936).
[40] M. CLAUSER and F. H. CLAUSER, *The Effect of Curvature on the Transition from Laminar to Turbulent Boundary Layer*, N.A.C.A. TN-613 (1937).
[41] H. W. LIEPMANN, *Investigations on Laminar Boundary Layer Stability and Transition on Curved Boundaries*, N.A.C.A. Wartime Rept. No. W-107 (1943).
[42] H. W. LIEPMANN, *Investigation of Boundary Layer Transition on Concave Walls*, N.A.C.A. Wartime Rept. No. W-87 (1945).
[43] L. BISSONNETTE and G. L. MELLOR, *Experiments on the Behaviour of an Axisymmetric Turbulent Boundary Layer with a Sudden Circumferential Strain*, J. Fluid Mech. *63*, 369–413 (1974).

Abstract

It has been shown that turbulent flows are greatly affected by streamline curvature. In spite of this and the fact that curved shear flows are frequently encountered in engineering applications, the predictions of such flows are relatively less developed than the predictions of two-dimensional plane flows. Recently, various attempts were made by different investigators; however, their methods are only successful when the product of the boundary layer thickness to the local surface curvature $|k\delta|$ is ~ 0.05. The present paper investigates the more general case where $0.1 \leq |k\delta| \leq 0.5$. Results show that the calculated boundary-layer characteristics for arbitrary free stream conditions are in good agreement with measurements.

Zusammenfassung

Es ist gezeigt worden, dass turbulente Strömungen durch eine stromlinienförmige Krümmung stark beeinflusst werden. Trotzdem und trotz der Tatsache, dass gekrümmte Randströmungen häufig bei technischen Anwendungen gefunden werden, sind die Vorhersagen solcher Strömungen verhältnismässig weniger entwickelt als die Vorhersagen zweidimensionaler ebener Strömungen. In letzter Zeit sind von verschiedenen Forschern Versuche in dieser Richtung unternommen worden; jedoch waren ihre Methoden nur dann erfolgreich, wenn das Verhältnis der Grenzschichtdicke zur bestimmten örtlichen Oberflächenkrümmung $|k\delta| \sim 0{,}05$ ist. Die vorgelegte Arbeit untersucht den allgemeineren Fall, bei dem $0{,}1 \leq |k\delta| \leq 0{,}5$ ist. Die Resultate zeigen, dass sich die berechneten Grenzschichteigenschaften für beliebig freie Strömungsbedingungen in befriedigender Uebereinstimmung mit den Messungen befinden.

(Received: March 29, 1977; revised: May 24, 1977)